International Conference on Mathematics, Computational Methods & Reactor Physics (M&C 2009)
Saratoga Springs, New York, May 3–7, 2009, on CD-ROM, American Nuclear Society, LaGrange Park, IL (2009)

EFFECTS OF THE TEMPERATURE DISCRETIZATION ON NUMERICAL METHODS FOR THERMAL RADIATION TRANSPORT

Ryan G. McClarren
Dept. of Nuclear Engineering
Texas A&M University
College Station, TX 77843-3133
rgm@tamu.edu

Robert B. Lowrie
Computational Physics and Methods Group
Los Alamos National Laboratory
P.O. Box 1663, MS D413, Los Alamos, NM 87545, USA
lowrie@lanl.gov

ABSTRACT

We present an analysis of three means of treating the material energy equation coupled with the nonlinear radiation transport equation in slab geometry. The radiation transport equation is discretized using a linear discontinuous Galerkin method. The material temperature is then treated with either 1) two temperature unknowns per cell, 2) one temperature unknown per cell, or 3) one temperature unknown per cell with a linear reconstruction of the emission source. Only the two temperatures per cell discretization is robust in the equilibrium diffusion limit. Though it is not robust in the diffusion limit, the reconstructed emission treatment is much more accurate than the one temperature per cell treatment. We use all three methods to solve a diffusive Marshak wave problem. These numerical solutions agree with the analysis. On a problem representing an ablating hohlraum where the solution is strongly influenced by a transport boundary layer between an optically thick and thin region, both the two temperature and reconstructed emission source treatments required 10 μm resolution to resolve the solution. The one temperature per cell solution was not yet converged at this fine resolution.

Key Words: thermal radiation transport, discontinuous Galerkin, transport effects

1. INTRODUCTION

Thermal radiation transport (also known as radiative transfer) problems are charactized by a wide variation of material properties. For example, regions of the problem where the material is cold can be entirely opaque and diffusive, whereas hot regions allow radiation to stream through. Due to the fact that the material temperature can change during a calculation, the behavior of radiation changes even within a spatial cell. Also, a further complication arises from the fact that the material can be transparent to high energy photons and opaque to low energy photons. Therefore, a numerical method for thermal radiation transport must adequately capture both the transport of the radiation when the cell is optically thin and the diffusive behavior when the cell is thick.

It has been well established that the discontinuous Galerkin method with linear elements, when used as a spatial discretization for transport problems, preserves the diffusion limit of the tranport equation for optically thick cells [1]. For two- and three-dimensional problems with quadrilateral cells, bilinear and trilinear

elements must be used to get the diffusion limit [2]—requiring four unknowns per radiation unknown (i.e. per each angular and energy unknown) per cell in the 2D case and eight such unknowns in the 3D case (up from two in the 1D case). This leporine proliferation of unknowns is even worse in problems of thermal radiation transport, where there is also a need for unknowns for the material temperature. In the past, schemes that have used a linear discontinuous Galerkin treatment for the material temperature have been shown to give the proper equilibrium diffusion limit [3–5]. This linear discontinuous method we shall refer to as the two temperature unknowns per cell method. Such schemes when extended to multidimensions, will then require more unknowns per spatial cell in the same manner as the radiation unknowns.

The purpose of this study is to look at different ways of coupling transport to the material equation with the goal of reducing the number of temperature unknowns required to get the equilibrium diffusion limit. On the surface such a reduction of unknowns might be possible because the material energy equation in the case of no material motion does not have a spatial derivative term. Additionally, when solving problems where radiation transport is coupled to hydrodynamics, the numerical methods generally preferred for hydrodynamics have only one temperature unknown per cell. In such a situation in order to couple a hydrodynamic method to a radiation method, one can have the radiation method separately store more temperature unknowns and use the input from the hydrodynamic method to adjust the average of the unknowns held by the radiation equations.

A middle ground that we explore in this study is using a single temperature unknown with a spatial reconstruction to compute blackbody emission sources at each cell edge. A reconstruction of the emission source has been used in implicit Monte Carlo calculations for years [6]. Such a recontruction is an example of a tradeoff between memory usage and computation: we have reduced the storage requirements of the scheme by adding a computation for the reconstruction step.

Below, we begin this work by introducing the linear discontinuous Galerkin method applied to the grey P_n equations in 1D slab geometry. Though we analyze 1D P_n , we note that our analysis applies directly to the 1D discrete ordinates equations when Gaussian quadrature is used. In section 3 we present three ways to treat the temperature unknown, followed by analysis of the diffusion limit of each in section 4. Section 5 presents our numerical results for both diffusive and transport-dominated problems. Then, in section 6 we present our conclusions.

2. LINEAR DISCONTINUOUS GALERKIN FOR THE 1D P_n EQUATIONS

The equations we are concerned with are the equation governing the transport of grey thermal radiation in slab geometry [7],

$$\frac{1}{c}\frac{\partial \psi}{\partial t} + \mu \frac{\partial \psi}{\partial x} + \sigma \psi = \frac{1}{2}\sigma a c T^4, \tag{1}$$

and an equation describing the change in material internal energy,

$$\frac{\partial e}{\partial t} = \sigma \left(\int_{-1}^{1} d\mu \, \psi - acT^4 \right). \tag{2}$$

In these equations $\psi(x, \mu, t)$ is the specific intensity of radiation, μ is the cosine of the direction-of-flight angle for a given particle, $\sigma(x, T)$ is the macroscopic cross-section of absorption, c is the speed of light, a is the radiation constant, $T(x, t)$ is the material temperature, acT^4 is the blackbody emission source, and e is the material internal energy. The material internal energy is related to the temperature through an equation

of state; if the material is stationary, as we assume in this study, we can write

$$\frac{\partial e}{\partial t} = C_{\mathrm{v}} \frac{\partial T}{\partial t}, \tag{3}$$

where C_{v} is the heat capacity at constant volume of the material and is defined by $C_{\mathrm{v}} \equiv \frac{\partial e}{\partial T}$. This form is desirable because the temperature dependence of the internal energy is explicit. Though we note that in cases where C_{v} is changing with temperature, this change must be accounted for to get a conservative time discretization.

One possible way to discretize the angular variable, μ, in Eq. (1) by expanding the μ dependence in Legendre polynomials and truncating the expansion at some order. The method, referred to as the P_n equations, is equivalent, in slab geometry, to the discrete ordinates method with Gaussian quadrature. The P_n equations are [5], for the system in Eqs. (1) – (2),

$$\frac{1}{c}\frac{\partial \psi_0}{\partial t} + \frac{\partial \psi_1}{\partial x} + \sigma\psi_0 = \sigma a c T^4 \quad l = 0, \tag{4a}$$

$$\frac{1}{c}\frac{\partial \psi_l}{\partial t} + \frac{l}{2l+1}\frac{\partial \psi_{l-1}}{\partial x} + \frac{l+2}{2l+1}\frac{\partial \psi_{l+1}}{\partial x} + \sigma\psi_l = 0 \quad 1 \le l \le n. \tag{4b}$$

The moments of the intensity, ψ_l, are defined by

$$\psi_l(x,t) = \int_{-1}^{1} P_l(\mu)\psi(x,\mu,t)\, d\mu, \tag{5}$$

where P_l is the l^{th} Legendre polynomial. To close the system, ψ_{n+1} is set to zero. The material energy equation only involves the zeroth moment of ψ,

$$C_{\mathrm{v}}\frac{\partial T}{\partial t} = \sigma\left(\psi_0 - acT^4\right). \tag{6}$$

It will be convenient for us to write the P_n equations as a linear hyperbolic system with a source,

$$\frac{1}{c}\frac{\partial \mathbf{\Psi}}{\partial t} + \mathbf{A}\frac{\partial \mathbf{\Psi}}{\partial x} = \mathbf{s}(\mathbf{\Psi}), \tag{7}$$

with

$$\mathbf{\Psi} = \begin{pmatrix} \psi_0 \\ \psi_1 \\ \psi_2 \\ \vdots \\ \psi_n \end{pmatrix}, \quad \mathbf{A} = \begin{pmatrix} 0 & 1 & \dots & \dots & \dots & \dots & 0 \\ \frac{1}{3} & 0 & \frac{2}{3} & \dots & \dots & \dots & 0 \\ 0 & \frac{2}{5} & 0 & \frac{3}{5} & \dots & \dots & 0 \\ \dots & \dots & \dots & \dots & \frac{n-1}{2n-1} & 0 & \frac{n}{2n-1} \\ \dots & \dots & \dots & \dots & \dots & \frac{n}{2n+1} & 0 \end{pmatrix}, \quad \mathbf{s}(\mathbf{\Psi}) = \begin{pmatrix} \sigma(acT^4 - \psi_0) \\ -\sigma\psi_1 \\ -\sigma\psi_2 \\ \vdots \\ -\sigma\psi_n \end{pmatrix}. \tag{8}$$

To discretize the system (7) in space we impose a spatial mesh of cells, each on the interval $[x_{m-1/2}, x_{m+1/2}]$ with $\Delta x_m = x_{m+1/2} - x_{m-1/2}$. Then we write the value of $\mathbf{\Psi}$ in cell m as

$$\mathbf{\Psi}_m(x,t) = \sum_{j=0}^{k} \mathbf{\Psi}_{m,j}(t) B_j(x). \tag{9}$$

Here $B_j(x)$ is a basis function on cell m and k is the number of basis functions. In this study we consider linear elements so that

$$B_1(x) = 1 - \frac{x - x_{m-1/2}}{\Delta x_m}, \qquad B_2(x) = \frac{x - x_{m-1/2}}{\Delta x_m}, \qquad \text{for } x \in [x_{m-1/2}, x_{m+1/2}]. \tag{10}$$

Note that $B_1(x)$ is one on the left edge of the cell and zero on the right, while $B_2(x)$ is zero on the left edge and one on the right.

We multiply the Eqs. (7) by B_j and integrate over a cell, this leads to the system,

$$\frac{1}{c}\mathbf{M}\frac{d}{dt}\begin{pmatrix}\mathbf{\Psi}_1\\ \mathbf{\Psi}_2\end{pmatrix} + \frac{1}{2}\begin{pmatrix}\mathbf{A}(\mathbf{\Psi}_1+\mathbf{\Psi}_2) - 2\mathbf{A}\mathbf{\Psi}_{m-1/2}\\ -\mathbf{A}(\mathbf{\Psi}_1+\mathbf{\Psi}_2) + 2\mathbf{A}\mathbf{\Psi}_{m+1/2}\end{pmatrix} = \mathbf{M}\begin{pmatrix}s_1\\ s_2\end{pmatrix}, \tag{11}$$

where we have dropped the $-_m$ subscript where possible, and we have assumed that $\mathbf{s}(\mathbf{\Psi})$ varies linearly over the cell. The mass matrix is given by

$$\mathbf{M} = \frac{\Delta x}{6}\begin{pmatrix}2\mathbf{I} & \mathbf{I}\\ \mathbf{I} & 2\mathbf{I}\end{pmatrix}, \tag{12}$$

where $\mathbf{I}$ is an $n+1 \times n+1$ identity matrix. Also, the source vector is

$$\mathbf{s}_j = \begin{pmatrix}\sigma(acT^4 - \psi_{0,j})\\ -\sigma\psi_{1,j}\\ \vdots\\ -\sigma\psi_{n,j}\end{pmatrix}, \tag{13}$$

where the means with which σ and T^4 are evalauted is unspecified. We also must specify the cell-edge fluxes, $\mathbf{A}\mathbf{\Psi}_{m\pm1/2}$. For these we use the "frozen" upwind flux [8, 9]

$$\mathbf{A}\mathbf{\Psi}_{m+1/2} = \frac{1}{2}\mathbf{A}\left(\mathbf{\Psi}_{m,2} + \mathbf{\Psi}_{m+1,1}\right) - \frac{1}{2}|\mathbf{A}|\left(\mathbf{\Psi}_{m+1,1} - \mathbf{\Psi}_{m,2}\right), \tag{14}$$

this is the solution of the free-streaming Riemann problem. Another way to write Eq. (11) is to multiply through by $\mathbf{M}^{-1}$ to get

$$\frac{1}{c}\frac{d}{dt}\begin{pmatrix}\mathbf{\Psi}_1\\ \mathbf{\Psi}_2\end{pmatrix} + \frac{1}{\Delta x}\begin{pmatrix}3\mathbf{A}(\mathbf{\Psi}_1+\mathbf{\Psi}_2) - 2\mathbf{A}\mathbf{\Psi}_{m+1/2} - 4\mathbf{A}\mathbf{\Psi}_{m-1/2}\\ -3\mathbf{A}(\mathbf{\Psi}_1+\mathbf{\Psi}_2) + 4\mathbf{A}\mathbf{\Psi}_{m+1/2} + 2\mathbf{A}\mathbf{\Psi}_{m-1/2}\end{pmatrix} = \begin{pmatrix}s_1\\ s_2\end{pmatrix}. \tag{15}$$

Equation (11) is the semi-discrete, linear discontinuous Galerkin discretization of the transport system in Eq. (7). In the next section we will discuss how the material energy equation, Eq. (6), can be discretized in space.

3. MATERIAL ENERGY DISCRETIZATION

To finalize our spatial discretization we need to treat the material energy equation. Perhaps the most natural way to discretize this equation is to have two temperature unknowns per cell,

$$C_\mathrm{v}(T_j)\frac{dT_j}{dt} = \sigma(T_j)\left(\psi_{0,j} - ac(T_j)^4\right), \qquad j = 1, 2. \tag{16}$$

This discretization is natural in the sense that there are two $\psi_{0,j}$ unknowns per cell and having two T_j's per cell allows the balance between ψ_0 and T^4 be enforced at each radiation unknown. The source term in this case is

$$\mathbf{s}_j = \begin{pmatrix} \sigma_j(acT_j^4 - \psi_{0,j}) \\ -\sigma_j\psi_{1,j} \\ \vdots \\ -\sigma_j\psi_{n,j} \end{pmatrix}, \tag{17}$$

with $\sigma_j = \sigma(T_j)$. It is worth noting that though having two temperatures per cell is a natural choice, this choice may not be easily available to transport method designer. In the case where the transport is coupled to a hydrodynamics calculation, in the so-called radiation hydrodynamics problems, the hydrodynamics calculation in general will have only one temperature unknown per cell. In such a case it is possible to have the radiation method save the previous time step slope in the cell and have hydrodynamics calculation update the cell average. Such a situation will not be analyzed in this study, but will be treated in future work.

In the case of one temperature unknown per cell, one could write the material equation using that one unknown and the average of ψ_0:

$$C_{\mathrm{v}}(T_m)\frac{dT_m}{dt} = \sigma(T_m)\left(\bar{\psi}_{0,m} - ac(T_m)^4\right), \tag{18}$$

where T_m is the temperature unknown for cell m and

$$\bar{\psi}_{0,m} = \frac{1}{2}\left(\psi_{0,m,1} + \psi_{0,m,2}\right). \tag{19}$$

Then, in this case the source term for the radiation equation is

$$\mathbf{s}_j = \begin{pmatrix} \sigma_m(acT_m^4 - \psi_{0,j}) \\ -\sigma_m\psi_{1,j} \\ \vdots \\ -\sigma_m\psi_{n,j} \end{pmatrix}. \tag{20}$$

Note that the source term in this case uses the same value of σ and T^4 for both radiation unknowns.

Another option for the case of one temperature unknown per cell is to reconstruct the T^4 emission term to get different edge values for this term. Reconstructing the source was suggested for implicit Monte Carlo by Fleck and Canfield [6]. A reconstruction that is compatible with the linear discontinuous radiation equation is

$$\tilde{T_1^4} = T_m^4 - \frac{1}{2}\Delta_{T^4}, \qquad \tilde{T_2^4} = T_m^4 + \frac{1}{2}\Delta_{T^4}, \tag{21}$$

where the slope Δ_{T^4} is computed as

$$\Delta_{T^4} = \Delta x_m \mathrm{minmod}\left(\frac{T_m^4 - T_{m-1}^4}{x_m - x_{m-1}}, \frac{T_{m+1}^4 - T_m^4}{x_{m+1} - x_m}\right), \tag{22}$$

with

$$\mathrm{minmod}(a,b) = \begin{cases} a & \text{for } |a| \le |b|, \text{ and } ab > 0 \\ b & \text{for } |a| > |b|, \text{ and } ab > 0 \\ 0 & \text{for } ab \le 0 \end{cases}. \tag{23}$$

This reconstruction scheme guarantees that the reconstructed T^4 is positive when all T's are positive and that the reconstructed T^4 is not an artificial local maximum or minimum. With the reconstruction the source is now

$$\mathbf{s}_j = \begin{pmatrix} \sigma_m(ac\tilde{T}_j^4 - \psi_{0,j}) \\ -\sigma_m\psi_{1,j} \\ \vdots \\ -\sigma_m\psi_{n,j} \end{pmatrix}. \tag{24}$$

Also, the discretized material energy equation is the same as in Eq. (18). The reconstruction scheme we suggest is conservative in the sense that

$$-\frac{1}{2}(\mathbf{s}_1 + \mathbf{s}_2) = \begin{pmatrix} \sigma(\bar{\psi}_{0,m} - acT_m^4) \\ \sigma_m\bar{\psi}_{1,j} \\ \vdots \\ \sigma_m\bar{\psi}_{n,j} \end{pmatrix} \tag{25}$$

implying that the source term in Eq. (18) is the same as zeroth element of the average of $\mathbf{s}_j$.

To make the analysis in the rest of this study more clear, we shall write $\mathbf{s}_j^{\text{ld}}$ as the source in Eq. (17), $\mathbf{s}_j^{\text{one}}$ as the source in Eq. (20), and $\mathbf{s}_j^{\text{recon}}$ as the source in Eq. (24).

4. DIFFUSION LIMIT ANALYSIS

For thermal radiation transport the equilibrium diffusion limit is an important case where the amount of absorption is large compared to the streaming of radiation. In this situation the radiation field and the emission term are in equilibrium to leading order, and the evolution of the material temperature is given by a nonlinear diffusion equation. Specifically, away from boundary and initial layers, to leading order the radiation transport system solves the nonlinear diffusion equation [10]

$$C_{\text{v}}\frac{\partial T}{\partial t} + a\frac{\partial T^4}{\partial t} = \frac{\partial}{\partial x}\frac{ac}{3\sigma}\frac{\partial T^4}{\partial x}, \tag{26}$$

with the radiation intensity in equilibrium with the emission term

$$\psi = \frac{1}{2}acT^4. \tag{27}$$

In this section we shall analyze the linear discontinuous Galerkin (LD) radiation treatment in the equilibrium diffusion limit coupled with the three different temperature treatments above.

The LD method has been throughly anaylzed for transport problems in the diffusion limit. Larsen and Morel [1] first showed that the method did possess the thick and thin diffusion limits for linear transport problems in slab geometry. For thermal radiation transport there have been several analyses of discontinuous Galerkin-type schemes with two temperature/internal energy unknowns per cell [3–5] and found that such schemes do possess the equilibrium diffusion limit. Here we shall briefly present a new analysis for the one temperature and reconstructed source equations and then compare it to the previously studied two temperature case.

To analyze the equilibrium diffusion limit we first introduce a small, positive parameter ϵ and make the replacements:

$$c \rightarrow \epsilon^{-1} c,$$
$$\sigma \rightarrow \epsilon^{-1} \sigma,$$
$$C_{\rm v} \rightarrow \epsilon C_{\rm v}.$$

When we make these scalings, in the limit of $\epsilon \rightarrow 0$ the mean-free path for a particle goes to zero, the particle speed goes to infinity, and the heat capacity goes to zero. We do note that the c in acT^4 is not scaled by ϵ^{-1} because that term is the result of integrating the Planck function over frequency, and the Planck function does not change in the diffusion limit.

4.1. Results from Two Temperature Unknowns Per Cell

Here we shall summarize the results of previous studies of the diffusion limit for the LD method with two temperature unknowns per cell. In this case the leading order solution satisfies for the case of σ and Δx constant [5]

$$\frac{1}{6}\left(C_{\rm v}\frac{dT_{m+1,2}}{dt} + 4C_{\rm v}\frac{dT_{m,2}}{dt} + C_{\rm v}\frac{dT_{m,1}}{dt}\right) + \frac{a}{6}\left(\left(T^4_{m+1,2}\right)^{(0)} + 4\left(T^4_{m,2}\right)^{(0)} + \left(T^4_{m,1}\right)^{(0)}\right) = \frac{ac}{3\sigma\Delta x^2}\left(\left(T^4_{m+1,2}\right)^{(0)} - 2\left(T^4_{m,2}\right)^{(0)} + \left(T^4_{m,1}\right)^{(0)}\right), \quad (28)$$

with the equilibrium between radiation and the emission source

$$\psi^{(0)}_{0,m,j} = ac\left(T^4_{m,j}\right)^{(0)}, \qquad j = 1, 2. \quad (29)$$

Equation (28) is an acceptable discretization of Eq. (26), indeed it is the continuous finite element discretization with piecewise linear elements.

4.2. One Temperature Unknown Per Cell

With the ϵ scaling, Eq. (11) becomes

$$\epsilon^2\frac{1}{c}\mathbf{M}\frac{d}{dt}\begin{pmatrix}\mathbf{\Psi}_1\\ \mathbf{\Psi}_2\end{pmatrix} + \epsilon\frac{1}{2}\begin{pmatrix}\mathbf{A}(\mathbf{\Psi}_1+\mathbf{\Psi}_2) - 2\mathbf{A}\mathbf{\Psi}_{m-1/2}\\ -\mathbf{A}(\mathbf{\Psi}_1+\mathbf{\Psi}_2) + 2\mathbf{A}\mathbf{\Psi}_{m+1/2}\end{pmatrix} = \mathbf{M}\begin{pmatrix}\mathbf{s}_1\\ \mathbf{s}_2\end{pmatrix}, \quad (30)$$

where in this case we use $\mathbf{s}^{\rm one}_j$. The material energy equation for the one temperature per cell case becomes

$$\epsilon^2 C_{\rm v}(T_m)\frac{dT_m}{dt} = \sigma(T_m)\left(\bar{\psi}_{0,m} - ac(T_m)^4\right), \quad (31)$$

We then postulate a power series expansion in ϵ of ψ, T, and T^4 of the form

$$(\cdot) = \sum_{k=0}^{\infty}(\cdot)^{(k)}\epsilon^k, \quad (32)$$

and then examine the scaled equations for like powers of ϵ. To leading order Eq.(30) is then

$$\begin{pmatrix}(\mathbf{s}^{\rm one}_1)^{(0)}\\ (\mathbf{s}^{\rm one}_2))^{(0)}\end{pmatrix} = \mathbf{0}, \quad (33)$$

and Eq. (31) is

$$\left(\bar{\psi}_{0,m}^{(0)} - ac\left(T_m^{(0)}\right)^4\right) = 0, \tag{34}$$

These equations imply that

$$\psi_{0,j}^{(0)} = ac\left(T_m^{(0)}\right)^4, \qquad j = 1,2 \tag{35}$$

$$\psi_{l,j}^{(0)} = 0, \qquad j = 1,2, \quad l > 0. \tag{36}$$

Therefore, to leading order $\psi_{0,j}$ is in equilibrium with the temperature in cell m.

To first order in ϵ Eqs. (30) becomes

$$\frac{1}{2}\begin{pmatrix} \mathbf{A}(\mathbf{\Psi}_1^{(0)} + \mathbf{\Psi}_2^{(0)}) - 2\mathbf{A}\mathbf{\Psi}_{m-1/2}^{(0)} \\ -\mathbf{A}(\mathbf{\Psi}_1^{(0)} + \mathbf{\Psi}_2^{(0)}) + 2\mathbf{A}\mathbf{\Psi}_{m+1/2}^{(0)} \end{pmatrix} = \mathbf{M}\begin{pmatrix} (\mathbf{s}_1^{\text{one}})^{(1)} \\ (\mathbf{s}_2^{\text{one}})^{(1)} \end{pmatrix}, \tag{37}$$

and the material energy equation implies that

$$\bar{\psi}_{0,m}^{(1)} = ac\left(T_m^{(1)}\right)^4. \tag{38}$$

Taking the $l = 0$ equations from the system in Eq. (37) we get that

$$|\mathbf{A}|_{00}\left(\psi_{0,m,1}^{(0)} - \psi_{0,m-1,2}^{(0)}\right) = \frac{\sigma\Delta x}{6}\left(ac\left(T_m^{(1)}\right)^4 - \psi_{0,m,1}^{(1)}\right), \tag{39}$$

$$-|\mathbf{A}|_{00}\left(\psi_{0,m+1,1}^{(0)} - \psi_{0,m,2}^{(0)}\right) = \frac{\sigma\Delta x}{6}\left(ac\left(T_m^{(1)}\right)^4 - \psi_{0,m,2}^{(1)}\right), \tag{40}$$

where $|\mathbf{A}|_{00}$ is the entry in row zero and column zero of $|\mathbf{A}|$. If we solve these equations for $\psi_{0,m,j}^{(1)}$, we get

$$\psi_{0,m,1}^{(1)} = ac\left(T_m^{(1)}\right)^4 - \frac{6|\mathbf{A}|_{00}}{\sigma\Delta x}\left(\psi_{0,m,1}^{(0)} - \psi_{0,m-1,2}^{(0)}\right), \tag{41a}$$

$$\psi_{0,m,2}^{(1)} = ac\left(T_m^{(1)}\right)^4 + \frac{6|\mathbf{A}|_{00}}{\sigma\Delta x}\left(\psi_{0,m+1,1}^{(0)} - \psi_{0,m,2}^{(0)}\right). \tag{41b}$$

Substituting Eqs. (41) into the left-hand side of Eq.(38) gives

$$\psi_{0,m+1,1}^{(0)} - \psi_{0,m,2}^{(0)} - \psi_{0,m,1}^{(0)} + \psi_{0,m-1,2}^{(0)} = 0, \tag{42}$$

which upon using the equilibrium condition in Eq. (35) yields

$$\left(T_{m+1}^{(0)}\right)^4 - 2\left(T_m^{(0)}\right)^4 + \left(T_{m-1}^{(0)}\right)^4 = 0. \tag{43}$$

Equation (43) states that to leading order the second-derivative of T^4 is zero—this is the so called zero resolution diffusion limit [2]. Clearly, this "diffusion" equation is not a valid discretization of Eq. (26).

4.3. Recontructed T^4

The analysis of the semi-discrete equations with $\mathbf{s}_j^{\text{recon}}$ begins in a similar fashion as the one temperature unknown per cell. The leading order equilibrium condition is

$$\psi_{0,j}^{(0)} = ac\left(\tilde{T}_j^{(0)}\right)^4, \qquad j = 1,2 \tag{44}$$

$$\psi_{l,j}^{(0)} = 0, \qquad j = 1,2 \quad l > 0. \tag{45}$$

Notice that $\psi_{0,j}^{(0)}$ is in equilibrium with the reconstructed value of the emission source, whereas before it was in equilibrium with the lone cell value of the emission source.

The reconstructed emission source case also leads to the equation

$$\psi_{0,m+1,1} - \psi_{0,m,2} - \psi_{0,m,1} + \psi_{0,m-1,2} = 0. \tag{46}$$

Substituting the value of $\psi_{0,j}^{(0)}$ from Eq. (44) into Eq. (46) yields

$$\left(T_{0,m+1}^{(0)}\right)^4 - 2\left(T_{0,m}^{(0)}\right)^4 + \left(T_{0,m-1}^{(0)}\right)^4 = \frac{1}{2}\Delta_{m+1,T^4}^{(0)} - \frac{1}{2}\Delta_{m-1,T^4}^{(0)}. \tag{47}$$

The only way that Eq. (47) does not lead to a zero resolution diffusion limit is if the relation reduces to $0 = 0$. However, there is no non-recursive way to define the slopes to make this the case*.

To show that the reconstruction does not lead to a reasonable diffusion limit, we will analyze Eq. (47) further. The Taylor expansion of any of the choices of how to compute the slope in Eq. (22) leads to

$$\frac{1}{2}\Delta_{m+1,T^4}^{(0)} - \frac{1}{2}\Delta_{m-1,T^4}^{(0)} = \frac{\Delta x^2}{2}\frac{\partial^2}{\partial x^2}\left(T^{(0)}\right)^4 + O(\Delta x^3), \tag{48}$$

where the error term can be $O(\Delta x^4)$ for a special choice of slope calculation. Substituting Eq. (48) into Eq. (47) and Taylor expanding the left-hand side gives

$$\frac{\partial^2}{\partial x^2}\left(T^{(0)}\right)^4 = O(\Delta x). \tag{49}$$

This restriction on the second derivative of T^4 is not compatible with the diffusion equation, and makes the solution approximately linear. Therefore, the reconstructed emission source does not give the diffusion limit. We note that the restriction on the second derivative in Eq. (49) is the same restriction that McClarren and Lowrie derived for the minmod slope limiter applied to the radiation variables [11].

If we continue the analysis to higher order in ϵ, we get as a final equation,

$$\frac{a}{6}\frac{d}{dt}\left(2\left(\tilde{T}_{m+1,1}^4\right)^{(0)} + \left(\tilde{T}_{m+1,2}^4\right)^{(0)} + \left(\tilde{T}_{m,1}^4\right)^{(0)} + 2\left(\tilde{T}_{m,2}^4\right)^{(0)}\right) = \frac{\sigma}{6}\left[ac\left(\tilde{T}_{m+1,1}^4\right)^{(2)} - 2\psi_{0,m+1,1}^{(2)} + ac\left(\tilde{T}_{m+1,2}^4\right)^{(2)} - \psi_{0,m+1,2}^{(2)} + ac\left(\tilde{T}_{m,1}^4\right)^{(2)} - \psi_{0,m,1}^{(2)} + 2ac\left(\tilde{T}_{m,2}^4\right)^{(2)} - 2\psi_{0,m,2}^{(2)}\right]. \tag{50}$$

This is clearly not a valid discretization of Eq. (26) as there is no spatial differencing term.

*It might be possible to define a recursive algorithm to relate Δ_{m+1,T^4} to Δ_{m-1,T^4}, though we do not analyze such schemes because we believe that they are not viable for multidimensional problems.

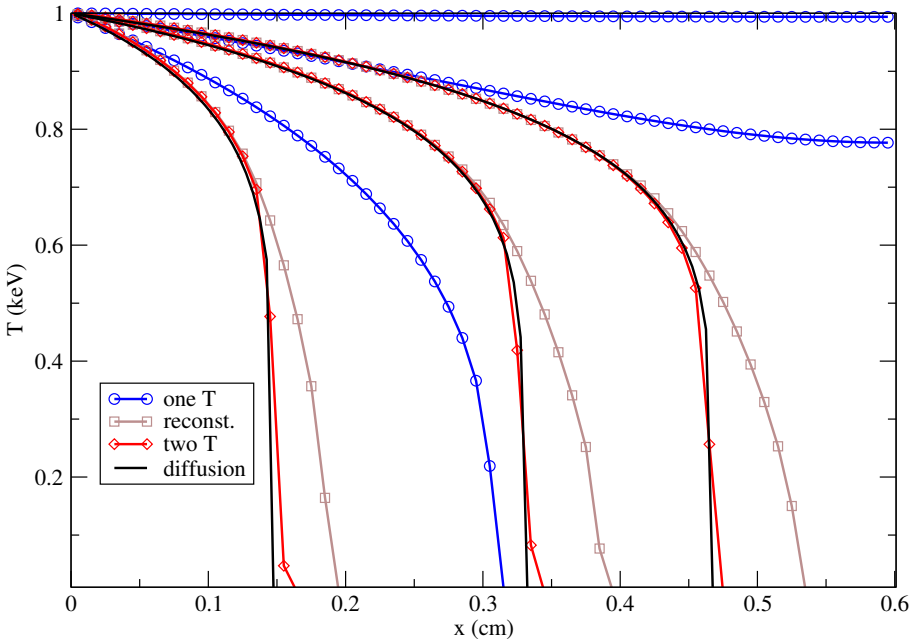

Figure 1. The material temperature from the different temperature discretizations compared to the equilibrium diffusion solution for the Marshak wave problem at $t = 10, 50, 100$ ns. The numerical solutions used $\Delta x = 0.01$ cm.

5. NUMERICAL RESULTS

Now we shall compare the three different treatments of the material temperature on several test problems. To solve the semi-discrete equations we use a semi-implicit scheme that updates the material interaction terms implicitly with a linearization of the emission term, and updates the streaming terms explicitly (for more detail see Ref. [5]). We perform each calculation with a CFL number of 0.3 and use the double minmod slope limiter to avoid artificial oscillations and preserve the diffusion limit [11].

The first problem we solve is a Marshak wave problem where our results from the analysis of the equilibrium diffusion limit should apply. This problem [5] has a spatial domain of $x \in [0, 0.6]$ cm with a 1 keV temperature source on the left boundary and a reflecting boundary on the left. The material properties are $\sigma = 300T^{-3}\,\text{cm}^{-1}$ with T measured in keV; the heat capacity is $C_\text{v} = 0.3 \times 10^{16}\,\text{erg/cm}^3\text{/keV}$. The initial condition is $T = 1.0 \times 10^{-6}$ keV with the radiation in equilibrium with the material. The numerical solutions from a P_3 calculation will be compared with the solution to the equilibrium-diffusion equation obtained by [12].

In Fig. 1 results for the different temperature treatments are shown. In this figure we notice that the one temperature per cell solution does not capture the diffusion solution at all; in fact, the 100 ns solution is a constant 1 keV throughout the problem. The two temperature per cell and reconstructed emission solutions agree with the equilibrium diffusion solution in the smooth region between the left boundary and the wave front. In this reqion the concavity of the solution is constant, therefore the reconstructed emission solution computes the slope in a consistent manner, giving an adequate diffusion discretization. However, only the two temperature solution can accurately capture the wave front. The recontructed emission solution smooths the wave front over several cells. This behavior at the wave front can be explained by the fact that the linear reconstruction in Eq. (22) is trying to make the solution linear in T^4, smoothing out the wavefront.

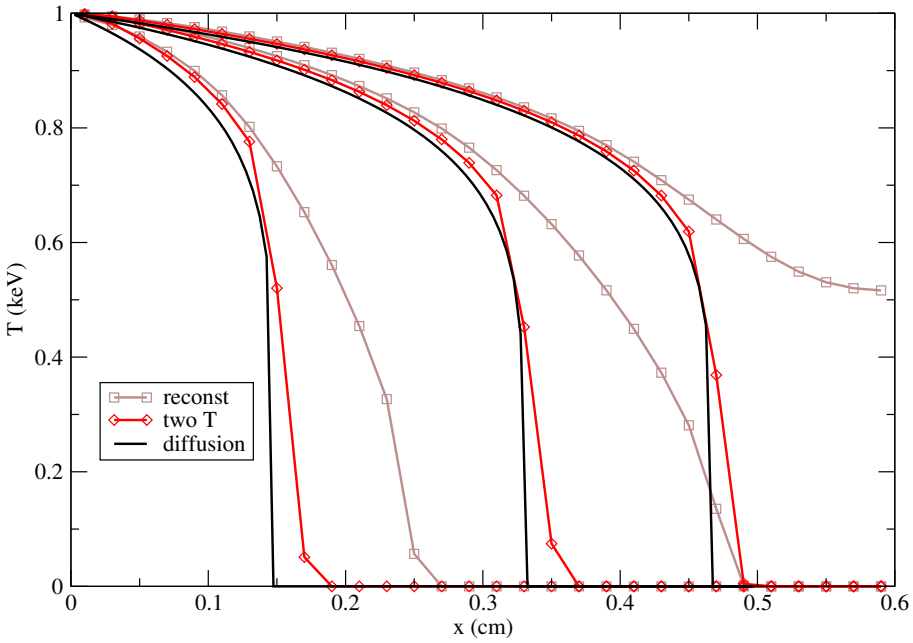

Figure 2. The material temperature for coarser spatial mesh from the reconstructed emission and two temperature discretizations compared to the equilibrium diffusion solution for the Marshak wave problem at $t = 10, 50, 100$ ns. The numerical solutions used $\Delta x = 0.02$ cm.

The behavior of the methods for a less resolved calculation are shown in Fig. 2. With this coarser mesh we do not show the one temperature solution because it already failed with a finer grid. The solution with the linear reconstruction of the emission source does a worse job of capturing the wave front. Again, the two temperature per cell solution captures the wave front as well as the grid resolution allows.

Another problem that we test the temperature discretizations on is a Marshak wave where the diffusion solution is not valid. In this problem $\sigma = 3T^{-3}$ with all other problem parameters the same. In this problem only the cold cells are optically thick, when a cell warms up it becomes optically thin. The solutions to this problem are shown in Fig. 3. These solutions all capture the fine mesh solution well and only differ slightly at the wave front.

The final test problem is meant to simulate gold ablating off of a hohlraum wall in an inertial confinement fusion experiment. The material is arranged with a density of $\rho = 10.78\,\mathrm{g/cm^3}$ from 0 to 1 cm and a density of $\rho = 0.1078\,\mathrm{g/cm^3}$ from 1 to 2 cm. The opacities are computed assuming that the gold is a fully ionized plasma using the bremsstrahlung absorption formula from Zel'dovich and Raizer [13]. The computed bremsstrahlung opacities in the thin and thick regions are

$$\sigma_{\text{thick}} = 657.4374T^{-7/2}\ \text{cm}^{-1}, \qquad \sigma_{\text{thin}} = 0.0657474T^{-7/2}\ \text{cm}^{-1}, \tag{51}$$

for T in keV.The heat capacities are $C_{\text{v}} = 0.5$ GJ/cm^3-keV in the thick region and $C_{\text{v}} = 10^{-4}$ GJ/cm^3-keV. Also, the initial temperatures are 1 keV in the thick region and 0.5 keV in the thin region. The boundary conditions have a 1 keV blackbody source at $x = 0$ and a reflecting boundary at $x = 2$ cm.

Figures 4 depict the numerical solution to this problem at 1 nanosecond. This problem has a thin boundary layer between the thick and thin regions: inside the thick region diffusion is an valid approximation but

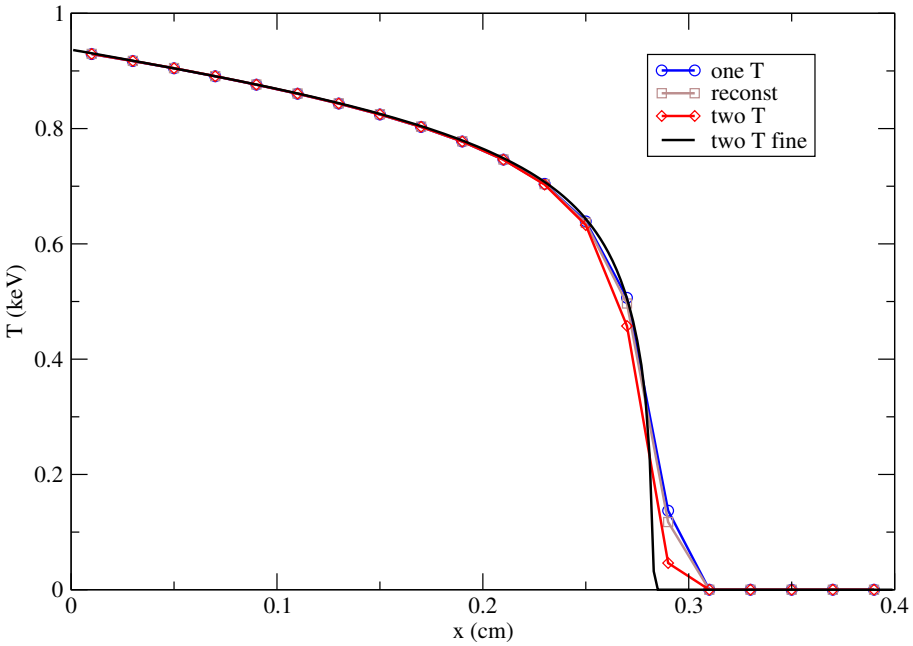

Figure 3. The material temperature for the thin Marshak wave using various temperature discretizations compared to a fine mesh calculation at $t = 1$ ns. The coase numerical solutions used $\Delta x = 0.01$ cm, whereas the fine solution used $\Delta x = 0.001$ cm.

there is a thin transition region between the thick and thin regions where the solution requires transport on a very short spatial scale to fully describe the physics. To converge on the correct solution for the temperature in the thin region, the two temperature and reconstructed emission source needed 2000 spatial cells or 10 μm resolution, despite the fact that away from the thin region the solutions for 1000 and 500 cells appear to the eye to be the same. A 4000 cell computation confirmed that the 2000 cell solutions were converged. The sensitivity of the temperature in the thin region can be explained by the fact that the thin region is so transparent to radiation that the rightmost unknown in the thick region completely determines the solution in the thin region. Therefore, the value of the transition region that this rightmost unknown has determines the temperature in the thin region; this behavior can be seen in Fig. 4(c).

The one temperature per cell solution is not yet converged with 2000 spatial cells. This is a result of the solution in the diffusion transition region not being converged. Also, note that this solution approaches the converged solution from above whereas the other two methods approach the solution from below. Perhaps surprisingly, it appears that the reconstructed emission source treatment gives better answers at the low resolutions than the two temperature per cell solutions. Though we point out that the slight difference between the 500 and 1000 cell solution from the reconstructed emission source could cause the uniniated user to conclude that the converged solution was the 1000 cell solution.

6 CONCLUSIONS

We have analyzed three different methods for discretizing the material temperature for slab geometry problems of nonlinear radiation transport. Only the two temperature per cell discretization is robust in the equilibrium diffusion limit; the one temperature per cell and the reconstructed emission source treatments fail to be robust in the diffusion limit. Our numerical results on a diffusive Marshak wave problem confirmed our

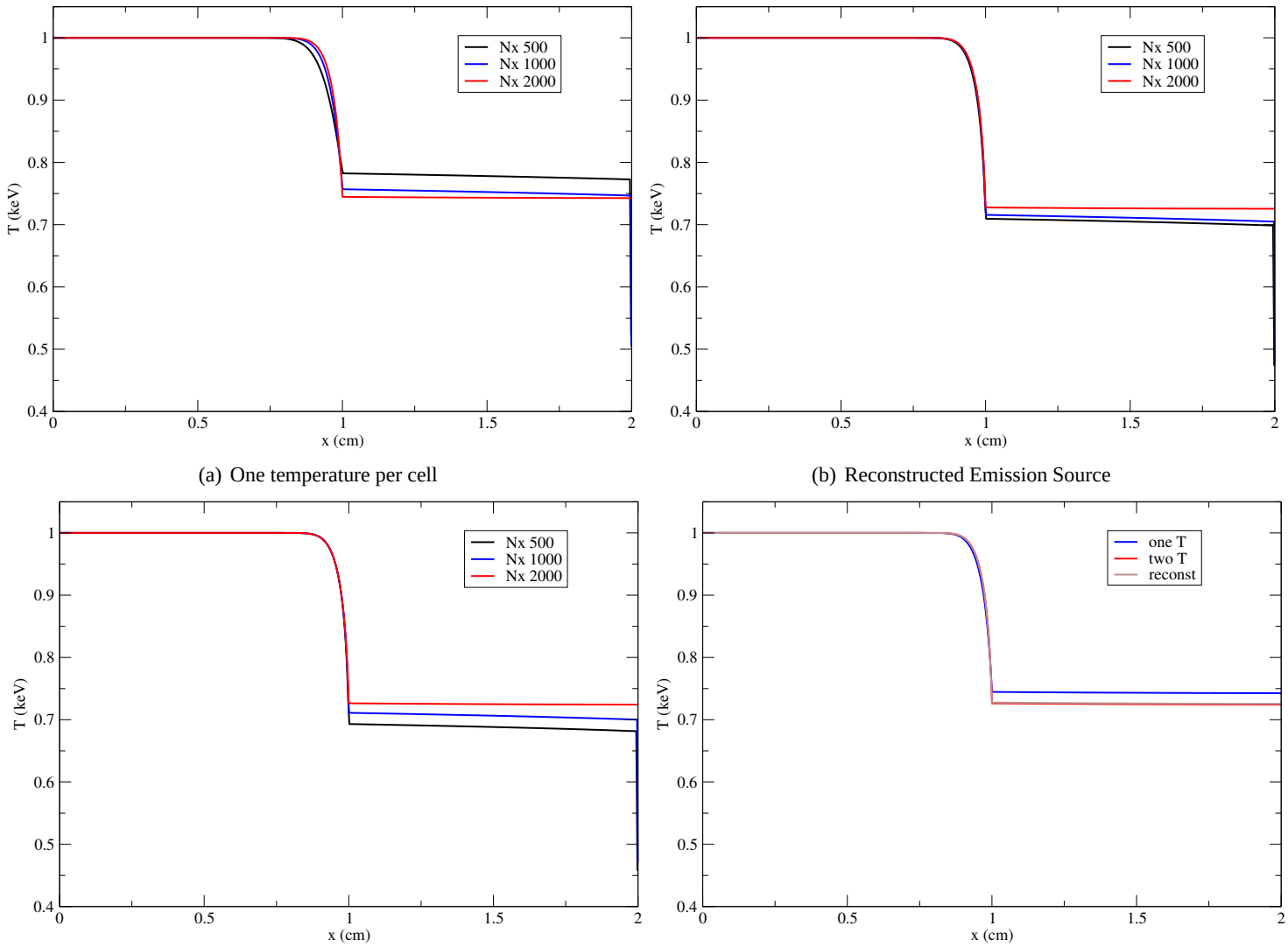

(a) One temperature per cell

(b) Reconstructed Emission Source

(c) Two temperatures per cell

(d) Comparison of Different Methods at N_x = 2000

Figure 4. Material temperature (keV) at 1 nanoseconds for the hohlraum problem using different temperature discretizations and the P_7 approximation. In these figures N_x is the number of spatial cells in the domain.

analysis. On a thin Marshak wave problem where only the material at the wavefront was diffusive, all the methods gave reasonable answers. Finally, in a problem strongly influenced by a transport boundary layer, both the two temperature and reconstructed emission solutions required 10 μm to resolved the solution; the one temperature cell solution was not yet converged at this fine resolution.

Our analysis has shown that simple means for reducing the temperature unknowns per cell will not give a method that is robust in the diffusion limit. We do not claim to have proven the null hypothesis that no treatment using one temperature unknown per cell is robust in the diffusion limit. We do assert that the two methods analyzed above do not work in the diffusion limit.

Finally, we believe that important future work will involve analyzing the coupling between a radiation method that requires two temperature unknowns per cell with a hydrodynamics method that has only one such unknown per cell.

ACKNOWLEDGMENTS

Portions of this work were performed under U.S. government contract DE-AC52-06NA25396 for Los Alamos National Laboratory, which is operated by Los Alamos National Security, LLC. (LANS) for the U.S. Department of Energy. LA-UR-08-06366.

R.G. McClarren's contribution to this publication is partially based on work supported by Award No. KUS-C1-016-04, made by King Abdullah University of Science and Technology (KAUST).

REFERENCES

[1] Edward W. Larsen and J. E. Morel. Asymptotic solutions of numerical transport problems in optically thick, diffusive regimes II. *J. Comp. Phys.*, 83:212–236, 1989.

[2] Marvin L. Adams. Discontinuous finite element transport solutions in thick diffusive problems. *Nucl. Sci. and Eng.*, 137:298–333, 2001.

[3] J. E. Morel, Todd A. Wareing, and Kenneth Smith. A linear-discontinuous spatial differencing scheme for S_n radiative transfer calculations. *J. Comp. Phys.*, 128:445–462, 1996.

[4] Marvin L. Adams and Paul F. Nowak. Asymptotic analysis of a computational method for time- and frequency- dependent radiative transfer. *J. Comp. Phys.*, 146:366–403, 1998.

[5] Ryan G. McClarren, Thomas M. Evans, Robert B. Lowrie, and Jeffery D. Densmore. Semi-implicit time integration for P_N thermal radiative transfer. *J. Comp. Phys.*, 227:7561–7586, 2008.

[6] J. A. Fleck, Jr. and E. H. Canfield. A random walk procedure for improving the computational efficiency of the implicit Monte Carlo method for nonlinear radiation transport. *Journal of Computational Physics*, 54:508–523, 1984.

[7] Gerald C. Pomraning. *The Equations of Radiation Hydrodynamics*. Pergamon Press, Oxford, 1973.

[8] R. B. Lowrie and J. E. Morel. Issues with high-resolution Godunov methods for radiation hydrodynamics. *J. Quantitative Spectroscopy and Radiative Transfer*, 69:475–489, 2001.

[9] Ryan G. McClarren, James Paul Holloway, and Thomas A. Brunner. On solutions to the P_n equations for thermal radiative transfer. *J. Comp. Phys.*, 227:2864–2885, 2008.

[10] E. W. Larsen, G. C. Pomraning, and V. C. Badham. Asymptotic analysis of radiative transfer problems. *Journal of Quantitative Spectroscopy and Radiative Transfer*, 29(4), 1983.

[11] Ryan G. McClarren and Robert B. Lowrie. The effects of slope limiting on asymptotic-preserving numerical methods for hyperbolic conservation laws. *J. Comp. Phys.* accepted Jul. 2008.

[12] T. M. Evans, T. J. Urbatsch, and H. Lichtenstein. 1-D equilibrium discrete diffusion Monte Carlo. In *Proceedings of the International Conference on Advanced Monte Carlo for Radiation Physics, Particle Transport Simulation, and Applications*, Lisbon, Portugal, October 2000.

[13] Ya. B. Zel'dovich and Yu. P. Raizer. *Physics of Shock Waves and High-Temperature Hydrodynamic Phenomena*. Dover Publications, Mineola, New York, 2002.